Comparison of the FFT Conjugate Gradient Method and the Finite-Difference Time-Domain Method for the 2-D Absorption Problem

DAVID T. BORUP, DENNIS M. SULLIVAN, AND OM P. GANDHI, FELLOW, IEEE

Abstract—**The need for high-resolution distributive dosimetry demands a numerical method capable of handling finely discretized, arbitrarily inhomogeneous models of biological bodies. At present, two of the most promising methods in terms of numerical efficiency are the fast-Fourier-transform conjugate gradient method (FFT-CGM) and the finite-difference time-domain (FD-TD) method. In this paper, these two methods are compared with respect to their ability to solve the 2-D lossy dielectric cylinder problem for both the TM and TE incident polarizations. Substantial errors are found in the FFT-CGM solutions for the TE case. The source of these errors is explained and a modified method is developed which, although inefficient, alleviates the problem and illuminates the difficulties encountered in applying the pulse-basis method of moments to biological problems. In contrast, the FD-TD method is found to yield excellent solutions for both polarizations. This, coupled with the numerical efficiency of the FD-TD method, suggests that it is superior to the FFT-CGM for biological problems.**

I. Introduction

In THE FIELD of bioelectromagnetics, there exists a need for numerical methods capable of computing high-resolution specific absorption rate (SAR) distributions in biological bodies exposed to RF electromagnetic fields. Applications include the quantification of environmental hazards (RF dosimetry) and the design and evaluation of hyperthermia applicators for the treatment of cancer. Numerical simulation of these problems requires algorithms capable of computing the resultant internal electric field induced inside an arbitrarily inhomogeneous lossy dielectric body exposed to a known incident electric field. Once the internal electric field ($|\bar{E}|$) is found, the specific absorption rate distribution ($\mathrm{SAR} = \frac{1}{2}\sigma|\bar{E}|^2$) can be computed. Analytic methods exist for the solution of simple geometries such as concentrically layered circular cylinders [1] and spheres [2], [3], and numerical methods have been developed for spheroids [4] and bodies of revolution [5]. The use of such methods is limited to the approximation of whole-body average SAR, layering effects, etc., due to the inability of these methods to take into account the complex external shape and internal structure of the human body.

A number of methods have been developed to deal with arbitrary inhomogeneity, and it is not the purpose of this paper to survey them all. Instead, this paper concentrates on two methods which we feel hold the most promise for handling high-resolution biological models due to their storage and computation efficiency. These are the fast-Fourier-transform conjugate gradient method (FFT-CGM) and the finite-difference time-domain (FD-TD) method. Here, these two methods are evaluated for their ability to solve the 2-D problem of an infinite lossy dielectric cylinder exposed to both TM and TE incident polarizations. Two-dimensional problems were chosen for two reasons. First, 2-D problems are less computationally involved than 3-D problems. This allows many test runs to be made for a variety of dielectric properties, frequencies, and cylinder sizes. Second, analytic solutions exist for homogeneous and coaxially layered circular cylinders illuminated by TM and TE incident plane waves. This allows a direct check on the accuracy to which the numerical methods can predict the internal electric fields.

The first method developed to solve the electric-field integral equation for the general 2-D dielectric cylinder was Richmond's [6], [7]. This approach uses the method of moments (MoM) with the pulse basis and point matching to discretize the integral equation into a linear system of equations that is then solved by matrix inversion. This method was extended to the general 3-D problem by Livesay and Chen [8] and has been applied to realistic models of man by Hagmann *et al.* [9]. A serious limitation of the traditional MoM is the need to invert a large matrix equation. This requires order N^3 computation and order N^2 storage, where N is the number of pulse-basis functions (cells) used to describe the body. This has limited the application of this method to relatively crude 180–1100-cell models [10].

In order to extend the resolution of the models that can be used in the integral equation method, Bojarski [11] developed the K-space method, which exploits the convolutional form of the electric-field integral equation by the use of the fast-Fourier-transform (FFT) algorithm.

Manuscript received August 27, 1986; revised November 26, 1986. This work was supported in part by the National Institute of Environmental Health Sciences, Research Triangle Park, NC, under Grant ES02304.

The authors are with the Department of Electrical Engineering, University of Utah, Salt Lake City, UT 84112.

IEEE Log Number 8612948.

This iterative approach reduces the storage and computation per iteration requirements to order N and $N\log_2(N)$, respectively. A related method, the stacked spectral iteration method (SSIT) of Kastner and Mittra [12], further reduces the computation requirement by decomposing the 3-D problem into a stack of 2-D problems. Difficulties associated with the convergence of these iterative methods prompted the development of the FFT-CGM [13], [14]. In this approach, the MoM with pulse basis and point matching is used to discretize the integral equation into a linear system that inherits the convolutional form of the integral equation. The linear system is then solved iteratively by the conjugate gradient method [15] using the discrete convolution theorem and the FFT algorithm to maintain order N storage and order $N\log_2(N)$ computation per iteration requirements.

A recent debate [16], [17] concerning the accuracy of pulse-basis MoM (PB-MoM) solutions has cast serious doubt on the applicability of this method to biological problems. Because the FFT-CGM is nothing more than an efficient means of solving the PB-MoM linear system, it is also suspect. It will be demonstrated in this paper that serious errors result when the FFT-CGM is applied to the 2-D lossy dielectric cylinder exposed to the TE incident polarization, while for the TM case, very accurate solutions are obtained. A major purpose of this paper is to explain the source of this problem by presenting a modified PB-MoM that provides excellent solutions for the TE case. Unfortunately this modified approach does not allow for the use of the FFT and thus requires order N^2 storage and order N^3 computations. In addition, the modified PB-MoM requires detailed modeling of all dielectric interfaces. This complicates the creation of the model considerably compared with the simple volume-averaged models that have been used. Nonetheless, the success of this method illuminates the source of the problems that have been encountered in the application of the PB-MoM and casts serious doubt on the solutions obtained in the past for simple block models of man.

The FD-TD method originated by Yee [18] and extended by Umashankar, Taflove, and Morris [19], [20] consists of solving a set of finite difference approximations to the time-dependent Maxwell's equations. The method enjoys significant advantages over the FFT-CGM in terms of computation and storage requirements and will be shown to provide excellent solutions for both the TM and TE polarizations. In addition, the FD-TD method does not require accurate modeling of the dielectric interfaces. The ability of this method to solve high-resolution biological models has been demonstrated in the application of the method to a realistic model of the isolated human eye [21]. Based on the results to follow, we feel that the FD-TD method is superior to the FFT-CGM for solving high-resolution bioelectromagnetic problems.

II. Description of the Methods

The FD-TD method consists of solving a set of finite difference approximations to the time-dependent Maxwell's equations. A plane wave, initially not touching the body, is propagated toward the body by time stepping with the finite difference equations. The wave is followed as it interacts with the body until the sinusoidal steady state is reached. Satisfaction of the radiation condition is equivalent to ensuring that the scattered field is not reflected back toward the body by the boundaries of the grid. This boundary condition is enforced by applying a finite difference operator at the grid boundary that selects outward-moving waves [22]. Use of this second-order-accurate boundary condition is claimed to ensure ± 2.5-percent uncertainty in the internal field magnitudes [20]. The FD-TD calculations presented in this paper were performed using a computer program provided by A. Taflove. A detailed description of the theory of the FD-TD method and the program can be found in [23].

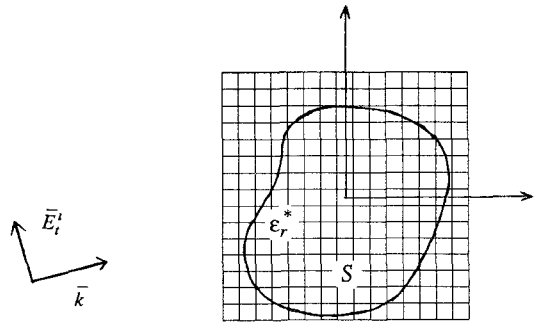

Fig. 1. Geometry of the 2-D TE cylinder problem and the constant increment discretization grid used in the FFT-CGM.

The FFT-CGM is described in [13] and [14] for the TM illumination of infinite dielectric cylinders and we derive here the method for the TE incident polarization. In Fig. 1, an infinite cylinder of arbitrarily inhomogeneous, lossy dielectric material of constant cross section S is illuminated by a TE-to-z incident field. From Maxwell's equations with $\exp(j\omega t)$ time dependence, the 2-D TE electric-field integral equation can be derived as in Harrington [24, p. 59]:

$$\bar{E}_t^i(\bar{\rho}) = \bar{E}_t(\bar{\rho}) + \frac{j}{4}k_0^2 \iint (\epsilon_r^*(\bar{\rho}') - 1)\bar{E}_t(\bar{\rho}') \cdot H_0^{(2)}(k_0|\bar{\rho} - \bar{\rho}'|)\, ds' + \frac{j}{4}\nabla \iint \nabla' \cdot [(\epsilon_r^*(\bar{\rho}') - 1)\bar{E}_t(\bar{\rho}')] \cdot H_0^{(2)}(k_0|\bar{\rho} - \bar{\rho}'|)\, ds' \quad (1)$$

where

$\bar{E}_t$ transverse total electric field,
$\bar{E}_t^i$ transverse incident electric field,
ϵ_r^* complex relative permittivity,
k_0 free-space propagation constant.

Suppose that the cross section is composed of N homogeneous subregions. The divergence of the polarization current in the second integral is zero inside such a region and impulsive at dielectric interfaces. This collapses the second integral into a line integral around all dielectric

interfaces, giving [33]

$$\bar{E}_t^i(\bar{\rho}) = \bar{E}_t(\bar{\rho}) + \frac{j}{4}k_0^2 \sum_{n=1}^{N} (\epsilon_n^* - 1) \cdot \int_{S_n} \int \bar{E}_t(\bar{\rho}') H_0^{(2)}(k_0|\bar{\rho} - \bar{\rho}'|)\, ds' - \frac{j}{4} \nabla \sum_{n=1}^{N} (\epsilon_n^* - 1) \cdot \int_{C_n} \bar{E}_t(\bar{\rho}') \cdot \hat{n}' H_0^{(2)}(k_0|\bar{\rho} - \bar{\rho}'|)\, dl' \quad (2)$$

where

ϵ_n^* complex relative permittivity of region n,
$\hat{n}$ outward-directed unit normal vector,
S_n surface area of region n,
C_n boundary of region n.

The FFT-CGM is based on the observation that the 2-D electric-field integral equation (1) has the form of a 2-D convolution integral. The idea is to discretize the equation in such a way as to preserve this form in the resulting linear system obtained by the application of the method of moments using the pulse basis and point matching. To this end, a square grid of constant increment Δ is placed over the surface S, as shown in Fig. 1. If the electric field and dielectric properties in each cell are assumed to be constant (pulse basis) and equality is enforced at the cell centroids (point matching), then there results from (2) the linear system of equations

$$\begin{bmatrix} E_x^i(n,m) \\ E_y^i(n,m) \end{bmatrix} = \begin{bmatrix} E_x(n,m) \\ E_y(n,m) \end{bmatrix} + \frac{j}{4}k_0^2 \sum_l \sum_k (\epsilon_{lk}^* - 1) \cdot \begin{bmatrix} E_x(l,k) \\ E_y(l,k) \end{bmatrix} \int_{S\Delta} \int H_0^{(2)} \cdot (k_0|\bar{\rho}_{nm} - \bar{\rho}_{lk} - \bar{\rho}'|)\, ds' - \frac{j}{4} \nabla \sum_l \sum_k (\epsilon_{lk}^* - 1) \begin{bmatrix} E_x(l,k) \\ E_y(l,k) \end{bmatrix} \cdot \int_{C\Delta} \hat{n}' H_0^{(2)}(k_0|\bar{\rho}_{nm} - \bar{\rho}_{lk} - \bar{\rho}'|)\, dl' \quad (3)$$

where

$S\Delta$ surface area of a cell centered at the origin,
$C\Delta$ boundary of $S\Delta$.

The linear system (3) is in the form of a 2-D discrete convolution since

$$|\bar{\rho}_{nm} - \bar{\rho}_{lk} - \bar{\rho}'| = \sqrt{((n-l)\Delta - x')^2 + ((m-k)\Delta - y')^2}. \quad (4)$$

In other words, since an equally spaced square grid has been used to discretize (1), the resulting linear system has inherited the convolutional form of the integral equation.

The first integral in (3) is approximated by replacing the square cell by a circle of equal area and evaluating the integral analytically. If the second integral is approximated in the same way, then the resulting method is equivalent to that originally used by Richmond [7] for the TE cylinder problem. It has been suggested by Hohmann [25] that the second integral should be evaluated by numerical quadrature along the square boundary. We have found, as discussed by Hagmann *et al.* [26] for the 3-D case, that subdivision of the cell into smaller cells and summing the Richmond approximations for these subcells converge to the values obtained by Hohmann's approach with less computational effort. This formulation is referred to in the literature [26] as the high-frequency Hohmann method (HFH) since it is a high-frequency modification of a method originally used by Hohmann [25] for geophysical problems.

Upon approximating the integrals in (3), the linear system can be written in the form

$$\begin{bmatrix} E_x^i(n,m) \\ E_y^i(n,m) \end{bmatrix} = \begin{bmatrix} E_x(n,m) \\ E_y(n,m) \end{bmatrix} + \sum_l \sum_k \begin{bmatrix} A(n-l,m-k), B(n-l,m-k) \\ B(n-l,m-k), C(n-l,m-k) \end{bmatrix} \cdot \begin{bmatrix} (\epsilon_{lk}^* - 1)E_x(l,k) \\ (\epsilon_{lk}^* - 1)E_y(l,k) \end{bmatrix}. \quad (5)$$

In this form, the linear system is clearly seen to be of the form of four coupled 2-D discrete convolutions. This form can be exploited by use of the discrete convolution theorem and the 2-D FFT algorithm to provide a means of computing the matrix product and its conjugate transpose in a number of operations proportional to $N \log_2(N)$ versus N^2 for direct summing, where N is the number of cells used to model the body. In addition, matrix storage is not needed since only the FFT's of the arrays A, B and C need to be stored. This reduces the storage requirement from order N^2 for traditional MoM to order N. This efficient means of computing the matrix products is then used to implement the conjugate gradient method (CGM) for the iterative solution of the linear system (5). This method of solving (5) introduces no additional error over more traditional methods such as LU decomposition since the convolutions in (5) can be computed without wrap-around aliasing by zero padding to twice the dimension of the scatterer [27, p. 110]. Recently, the CGM has become a popular means for solving linear systems encountered in the application of the MoM [28]–[30]. In these methods, the convolutional property of the linear system is not exploited by use of the FFT algorithm, and as a result, these methods require order N^2 computations per iteration and order N^2 storage. It should be mentioned that the CGM approach proposed by Sultan and Mittra [30] requires order N^2 computations but a storage requirement proportional to N since the matrix elements are extracted from a lookup table as needed.

Table I summarizes the storage and computation requirements of the FFT-CGM and the FD-TD method for the TE case. The FD-TD requires about 10 percent of the

TABLE I
STORAGE AND COMPUTATION COMPARISON FOR THE 2-D TE CASE

	FFT-CGM	FD-TD
Multiplies	$64N \log_2(N)$	$2N$
Adds	$64N \log_2(N)$	$10N$
Storage	$64N$	$7N$

Computations for the FFT-CGM are for one CGM iteration. The FD-TD values are for one time step. N is the number of cells used in the model.

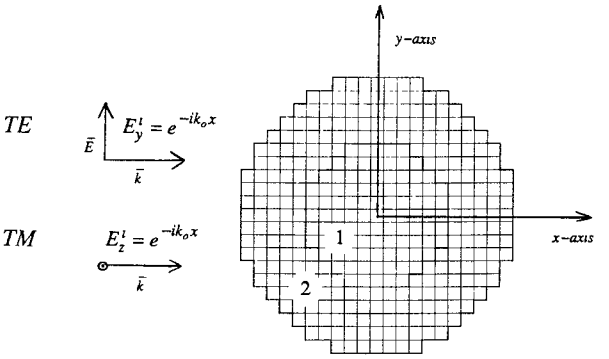

Fig. 2. Geometry of the layered circular cylinder test case. Outer layer radius = 15 cm, inner layer radius = 7.9 cm.

storage needed by the FFT-CGM. Also, considerably less computation per iteration is needed for the FD-TD method. The comparison presented in Table I is not entirely accurate since the computations for the FFT-CGM are for one conjugate gradient iteration while the values for the FD-TD are for one time step. For the test cases to follow, the number of iterations and time steps needed will be given for a more accurate comparison of the methods.

III. TEST CASES

Fig. 2 illustrates the model used in the test cases that follow. A coaxially layered circular cylinder is modeled by a 21×21 square grid with an inner layer defined by an 11×11 grid for a total of 349 cells. Also shown are the TM and TE incident plane wave polarizations considered. Fig. 3 compares the results obtained with the FFT-CGM and the FD-TD method for the case of a homogeneous muscle tissue cylinder exposed to a 100-MHz TM polarized plane wave of amplitude 1 V/m. The values for the dielectric properties of biological tissue were taken from [31]. The solutions are compared with the exact solution along the x axis from front to back and on the y axis from the center to the top of the cylinder (the solution is symmetric in y). The exact solution represented by the continuous line was computed analytically as described in [32]. Both numerical solutions agree favorably with the exact solution for this case.

Fig. 4 shows the results for a two-layer cylinder with an inner layer of muscle and an outer layer of fat for an incident frequency of 100 MHz. Fig. 5 shows the comparison for a homogeneous muscle cylinder for a frequency of 300 MHz. For these cases also, both methods agree well with the exact solution.

The TM results displayed here represent only a small sample of the cases that have been considered. We have found that both methods give good solutions for the TM polarization for a wide variety of layering geometries and frequencies up to 1 GHz. The sampling density required to obtain an accurate solution is on the order of five to ten samples per internal wavelength.

Fig. 6 compares the two methods for the case of a 100-MHz TE polarized incident plane wave illuminating a homogeneous muscle cylinder. As before, the methods are compared with the exact solution along the x and y axes. The E_x field is zero on the x axis due to symmetry. For this case, the FD-TD solution agrees very favorably with the exact solution. In contrast, severe errors are present in the FFT-CGM solution. Notice the erratic behavior of the solution in general and in particular the large errors in the tangential components at the air–dielectric interface.

Fig. 7 shows the TE results obtained for the muscle–fat layered case. An interesting feature of this case is the fact that both methods correctly predict the jump discontinuity in E_y along the y axis. As before, the FD-TD solution is superior to the FFT-CGM solution. As in the homogeneous case, the FFT-CGM solution is not as smooth as the FD-TD solution, and there is considerable error in the tangential component of the solution at both dielectric interfaces. Notice that the FFT-CGM method predicts large discontinuities in the tangential component of the field at dielectric interfaces. Fig. 8 shows the comparison for the 300-MHz homogeneous case. Again the FD-TD solution agrees very well with the exact solution. Very large errors are seen for the FFT-CGM solution. Notice the very erratic, oscillatory behavior of the computed E_y field on the x axis. An explanation of this behavior will be given shortly.

TABLE II
ITERATION AND COMPUTATION REQUIREMENTS FOR THE TEST PROBLEMS OF FIGS. 3–8

Frequency and Polarization	Fig.	FFT-CGM Iterations	FFT-CGM Operations $\times 10^{-6}$	FD-TD Time-steps	FD-TD Operations $\times 10^{-6}$
100 MHz TM Homogeneous	Fig.3	4	1.8	1500	18.4
100 MHz TM Layered	Fig.4	5	2.3	1500	18.4
300 MHz TM Homogeneous	Fig.5	9	4.1	300	3.7
100 MHz TE Homogeneous	Fig.6	300	550	1500	18.4
100 MHz TE Layered	Fig.7	300	550	1500	18.4
300 MHz TE Homogeneous	Fig.8	300	550	300	3.7

The operations values are the sum of the real adds and real multiplies.

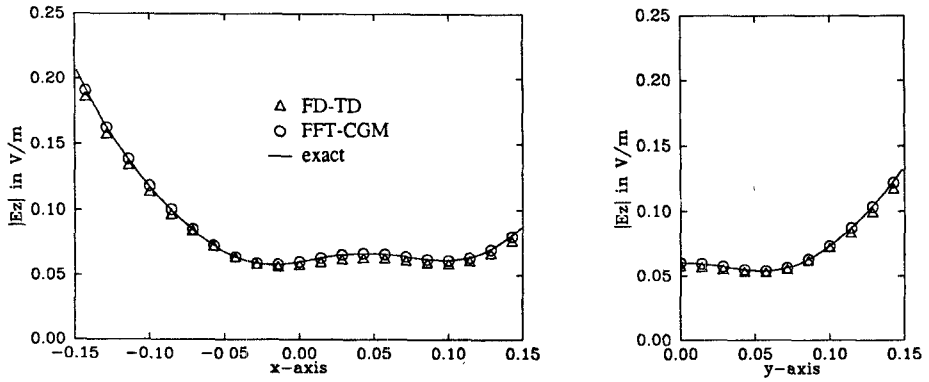

Fig. 3. TM test case no. 1. Homogeneous muscle cylinder. Frequency = 100 MHz; $\epsilon_{r1} = \epsilon_{r2} = 72$; $\sigma_1 = \sigma_2 = 0.9$ S/m.

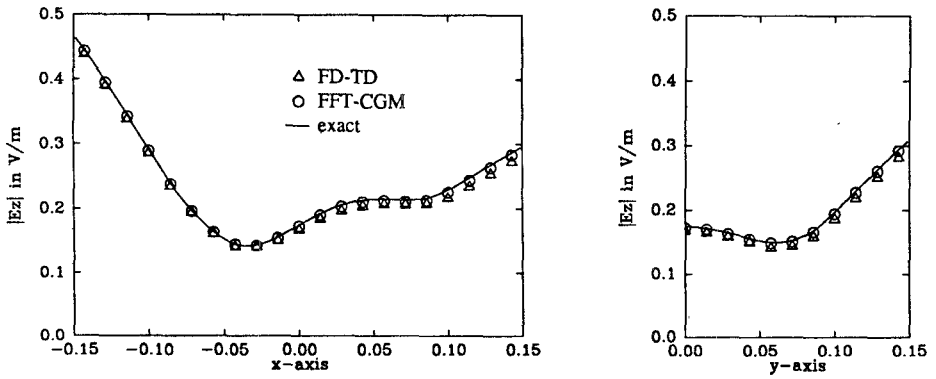

Fig. 4. TM test case no. 2. Layered muscle–fat cylinder. Frequency = 100 MHz; $\epsilon_{r1} = 72$, $\epsilon_{r2} = 7.5$; $\sigma_1 = 0.9$ S/m, $\sigma_2 = 0.048$ S/m.

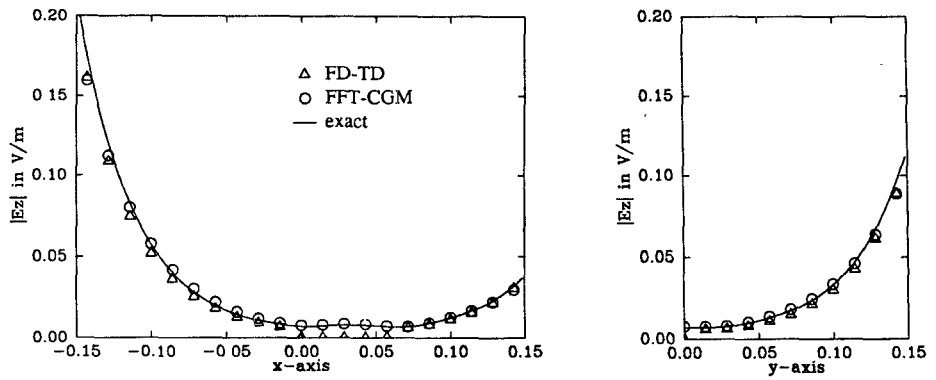

Fig. 5. TM test case no. 3. Homogeneous muscle cylinder. Frequency = 300 MHz; $\epsilon_{r1} = \epsilon_{r2} = 54$; $\sigma_1 = \sigma_2 = 1.4$ S/m.

Table II displays the number of FFT-CGM iterations and FD-TD time steps and the total number of real operations required to obtain the solutions of Figs. 3–8. For numerical stability of the FD-TD iterations, the time step duration δ_t must satisfy

$$\delta_t \leq \frac{\delta_x}{2C_0}$$

where δ_x is the cell size and C_0 is the velocity of light. For adequate convergence to the steady state, the passage of two to three wavelengths is required and so the total number of time steps needed (for 2.5 wavelengths) is

$$N \geq \frac{5\lambda}{\delta_x}.$$

Thus, the number of time steps needed for convergence is inversely proportional to the electrical size of the cell. For this reason, the FD-TD method requires fewer time steps as the frequency is increased for a given cell size.

While the number of time steps required for the FD-TD method to converge is known *a priori* from simple considerations, the number of iterations required for the FFT-CGM is not so well defined. For the TM case, the CGM

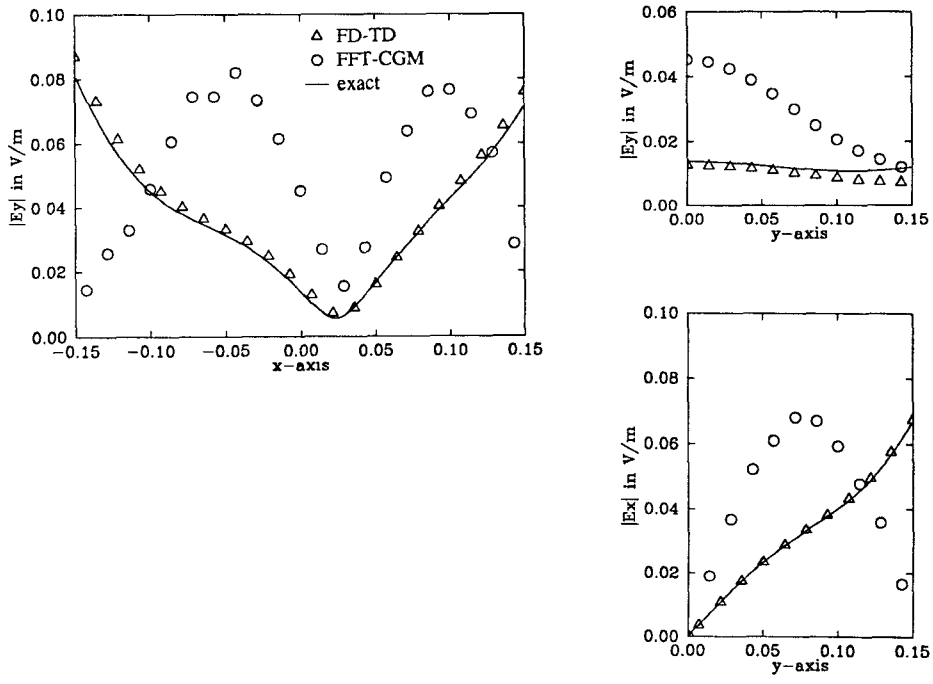

Fig. 6. TE test case no. 1. Homogeneous muscle cylinder. Frequency = 100 MHz; $\epsilon_{r1} = \epsilon_{r2} = 72$; $\sigma_1 = \sigma_2 = 0.9$ S/m.

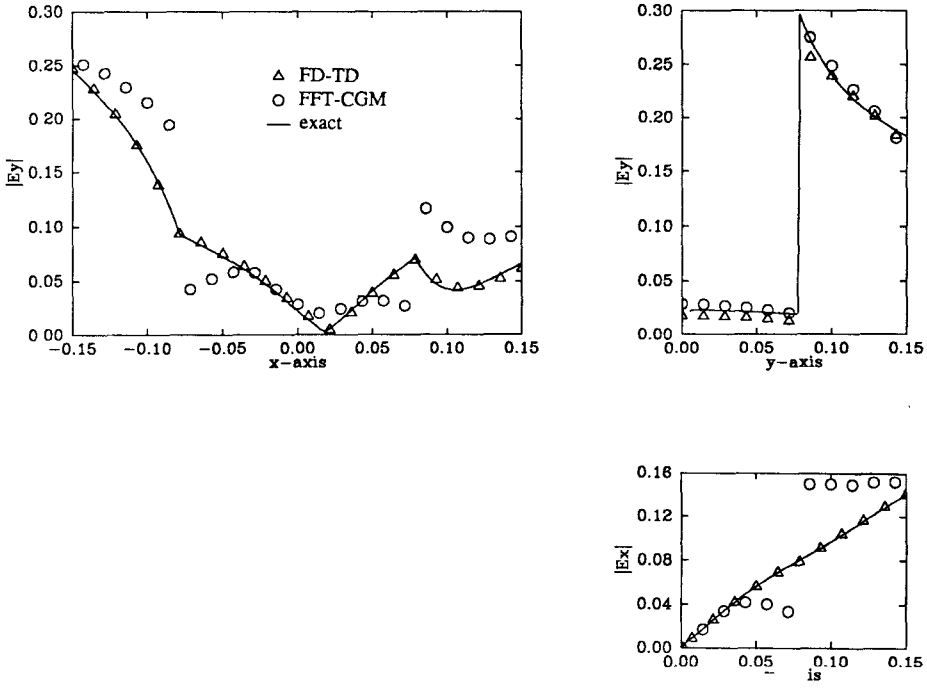

Fig. 7. TE test case no. 2. Layered muscle–fat cylinder. Frequency = 100 MHz; $\epsilon_{r1} = 72$, $\epsilon_{r2} = 7.5$; $\sigma_1 = 0.9$ S/m, $\sigma_2 = 0.048$ S/m.

converges very rapidly in far fewer iterations than the number of unknowns, making the FFT-CGM competitive with the FD-TD for this polarization. For the TE case, however, the CGM requires a number of iterations on the order of the number of unknowns. It is well known that the number of iterations needed for convergence of the CGM is equal to the number of independent eigenvalues of the matrix [28]. Apparently, many of the eigenvalues of the TM matrix are degenerate or nearly so, resulting in very rapid convergence. For the TE matrix, it appears that the eigenvalues are mostly independent, thus, the number of iterations required is on the order of the number of unknowns. This, coupled with the greater computation per iteration required, makes the FFT-CGM much less efficient than the FD-TD method for the 2-D TE and, presumably, the 3-D cases.

In order to shed some light on the convergence problems encountered in the use of the pulse-basis MoM approach to the TE problem, a series of increasingly finer discretizations of the type shown in Fig. 2 were considered. Fig. 9

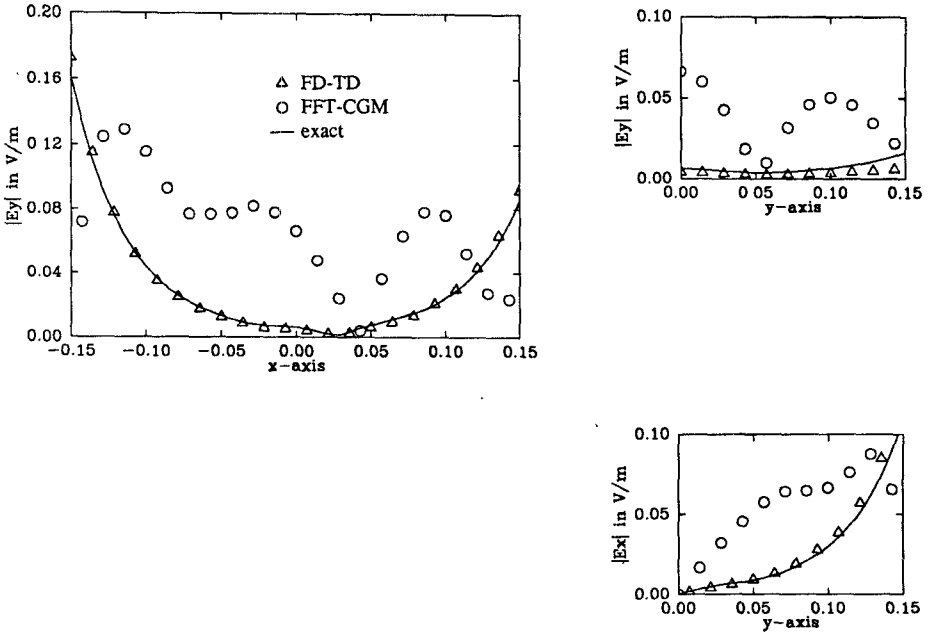

Fig. 8. TE test case no. 3. Homogeneous muscle cylinder. Frequency = 300 MHz; $\epsilon_{r1} = \epsilon_{r2} = 54$; $\sigma_1 = \sigma_2 = 1.4$ S/m.

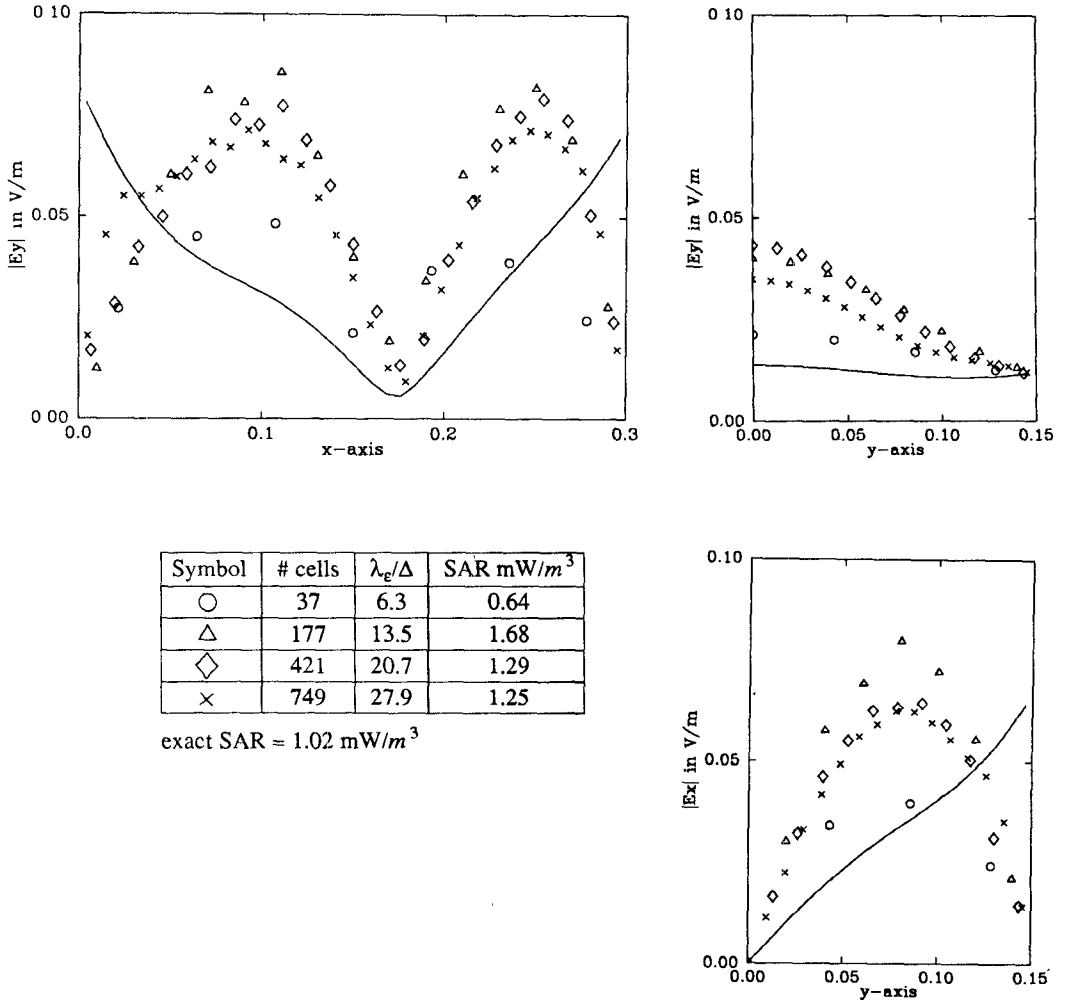

Symbol	# cells	λ_g/Δ	SAR mW/m^3
○	37	6.3	0.64
△	177	13.5	1.68
◇	421	20.7	1.29
×	749	27.9	1.25

exact SAR = 1.02 mW/m^3

Fig. 9. Discretization series test cases for the FFT-CGM. Frequency = 100 MHz, radius = 15 cm, $\epsilon_r = 72$, $\sigma = 0.9$ S/m.

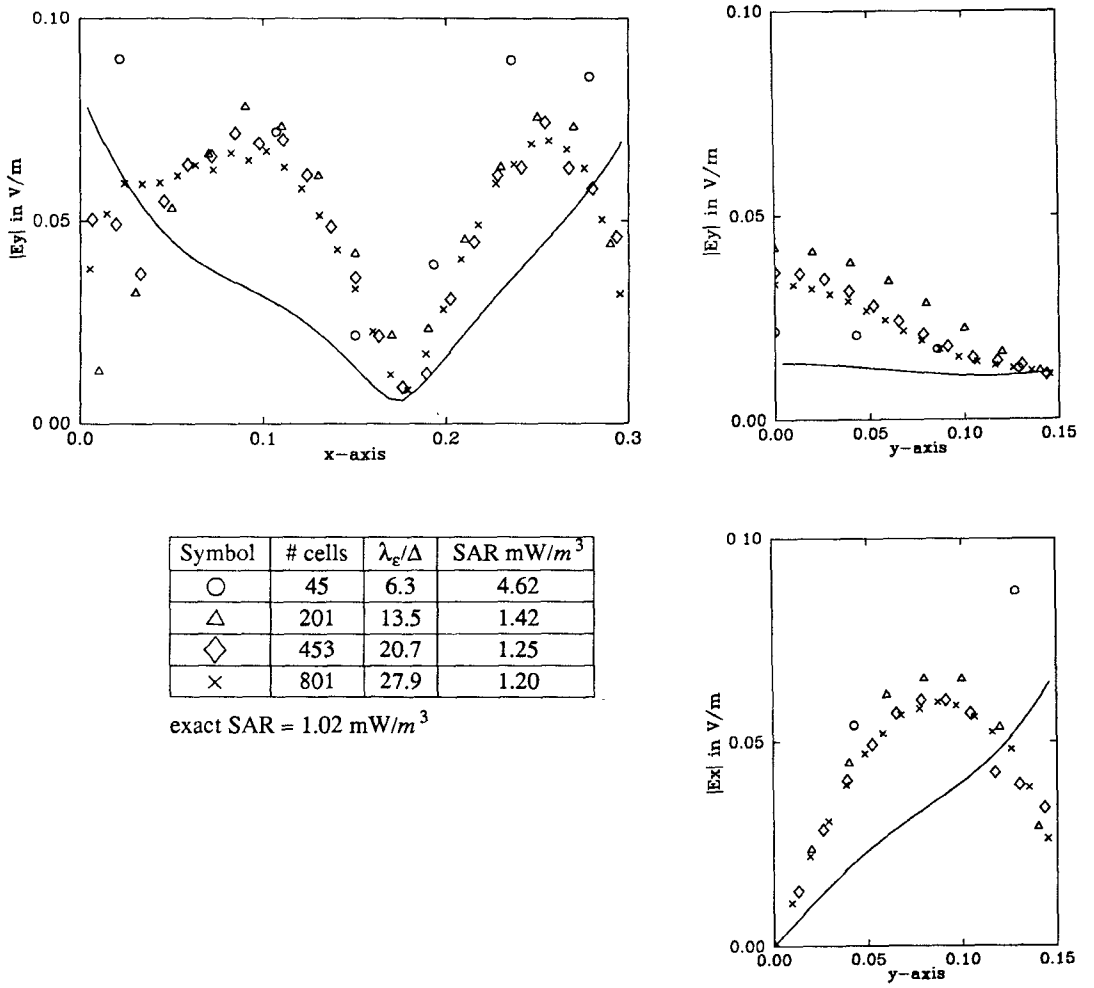

Symbol	# cells	λ_ϵ/Δ	SAR mW/m^3
○	45	6.3	4.62
△	201	13.5	1.42
◇	453	20.7	1.25
×	801	27.9	1.20

exact SAR = 1.02 mW/m^3

Fig. 10. Volume-averaged discretization series test cases for the FFT-CGM. Frequency = 100 MHz, radius = 15 cm, $\epsilon_r = 72$, $\sigma = 0.9$ S/m.

shows the results obtained for 37, 177, 421, and 749 cell block models of a homogeneous circular cylinder of muscle tissue exposed to a 100-MHz TE plane wave. As the number of cells is increased, the model is refined in the sense that the surface area of the model converges to the area of the circular cross section. Note, however, that the arc length and shape of the boundary do not converge to that of the circular cylinder for increasingly finer discretizations. This inaccurate modeling of the air–dielectric interface will be shown in the next section to be the cause of the errors encountered in the previous TE solutions.

It might be suggested that more rapid convergence of the model geometry and correspondingly better solutions might be obtained by replacing the block model of Fig. 2 with an air–dielectric volume-averaged model. In Fig. 2, a cell was considered to be either entirely inside or outside the body, and it could be argued that this reinforces the jagged shape of the model boundary. A different approach would be to assign to each cell a dielectric constant corresponding to the average dielectric constant enclosed by the volume of the cell. This volume-averaging approach is actually what has been used in practice. For example, the 180-cell man model developed by Hagmann *et al.* [9] is a volume-averaged model. To test the effect of this modification, volume-averaged models for the TE problems of Fig. 9 were considered. Fig. 10 shows the results obtained using volume averaging. These solutions differ only slightly from those of Fig. 9. The characteristics and magnitude of the error in the volume-averaged solutions are essentially the same as for the model of Fig. 2. Thus, we find no benefit in this modification.

Careful examination of Figs. 9 and 10 reveals several interesting features of the block model MoM solutions. Notice that as the number of cells is increased, the solution tends to converge to a final shape. In addition, the whole-body average SAR tends to converge to a value about 25 percent larger than the exact value. Although the MoM solutions do appear to converge to a final shape and the SAR seems to converge to a value close to the correct one, the solutions deviate significantly from the exact solution in terms of the interior distribution even though the sampling density has reached 28 samples per internal wavelength. This result indicates that the apparent convergence of the whole-body average SAR is not an indication that the internal SAR distribution is accurate.

The source of the overall roughness of the solutions in Figs. 9 and 10 can be explained by considering the results

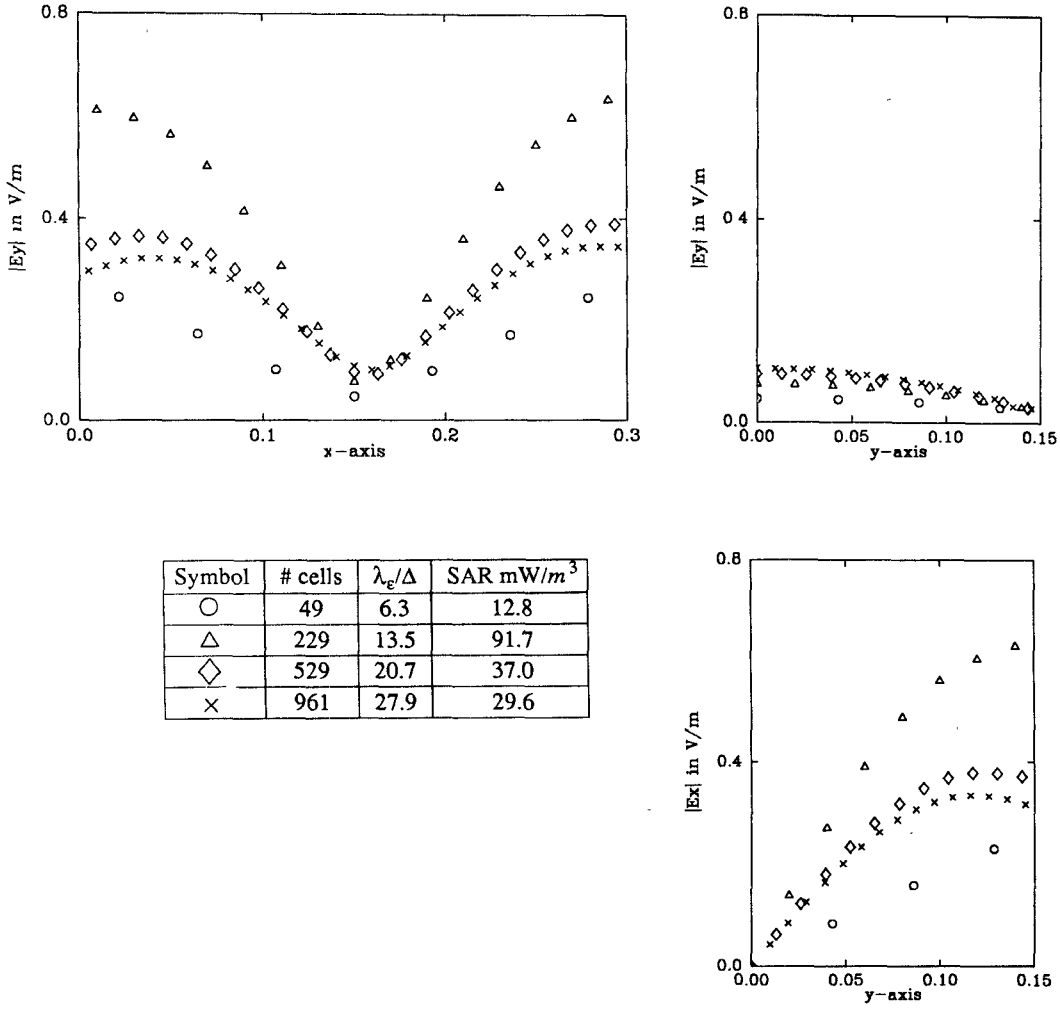

Symbol	# cells	λ_e/Δ	SAR mW/m^3
○	49	6.3	12.8
△	229	13.5	91.7
◇	529	20.7	37.0
×	961	27.9	29.6

Fig. 11. Square cylinder discretization series test cases for the FFT-CGM. Frequency = 100 MHz, width = 30 cm, $\epsilon_r = 72$, $\sigma = 0.9$ S/m.

in Fig. 11 for square cylinders. The only difference between the models used in Fig. 11 and Fig. 9 is that the circular cylinder block models have been filled out into squares—a shape that the square-cell block models fit exactly in area, boundary shape, and boundary length. Notice that the MoM solutions are now very smooth. Clearly, the source of much of the erratic behavior of the previous TE results is due to the inaccurate modeling of the dielectric boundary by the block models. To see why this is true, consider (2) for the case of a single homogeneous region. The second integral in this equation becomes a single line integral about the boundary of the body. This suggests that the integral equation solution is very sensitive to the accuracy of the boundary representation. Block models, such as Fig. 2, converge in terms of surface area as the number of cells is increased but the arc length and shape of the boundary does not. The second integral in (2) is an integration of the polarization charge at the interface between two different dielectrics. It is this charge that accounts for the jump discontinuity in the normal component of the electric field at such an interface; thus, the geometry of the boundary must be modeled accurately to ensure proper satisfaction of this boundary condition.

The shortcomings of the pulse-basis MoM applied to the TE-illuminated dielectric cylinder were first pointed out by Harrington [24, p. 59] in a discussion of the results obtained by Richmond [7] for the TE cylinder problem. Harrington suggested that the errors encountered in computing the scattered power pattern of a coaxial dielectric shell were due to the fact that the pulse-basis function is not in the domain of the TE integro-differential operator. He further suggested that the pulse-basis solution should not be expected to converge to the exact solution as the number of pulses describing the cylinder is increased. In the next section, it will be shown that convergence can in fact be obtained with the pulse basis if the cell structure of the model is carefully designed and the matrix elements are evaluated correctly.

A number of alternative formulations have been suggested to alleviate these difficulties. These approaches generally involve the use of higher order basis functions, e.g. linear and rooftop functions. Hill *et al.* [33] developed a linear basis Galerkin method for a quasi-static approximation to the TE electric-field integral equation. This approach was found to yield excellent solutions for homogeneous and coaxially layered cylinders of biological tissue.

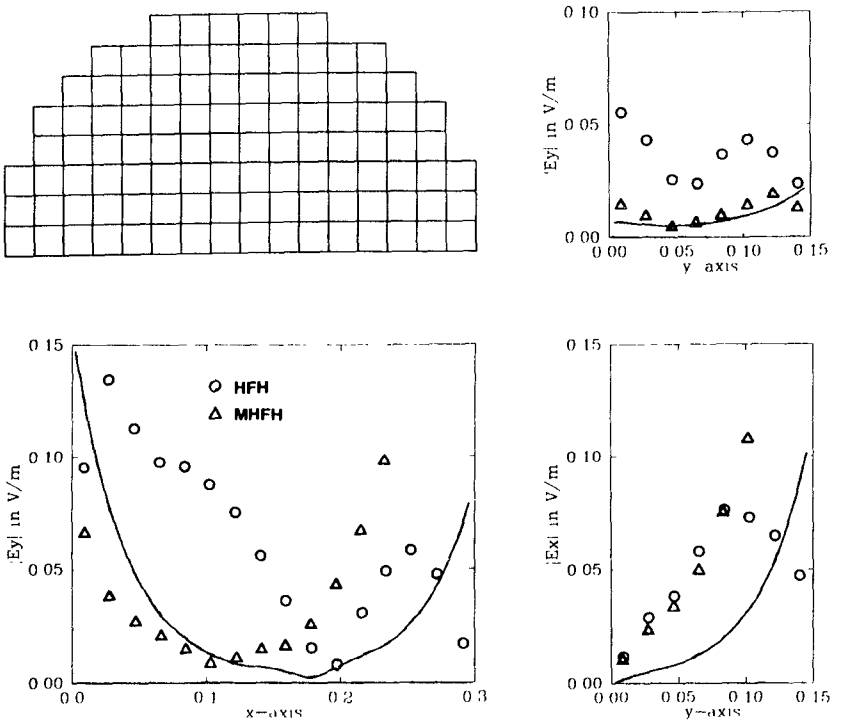

Fig. 12. Block model HFH and MHFH solutions versus the analytic solution. Frequency = 300 MHz, radius = 15 cm, $\epsilon_r = 54$, $\sigma = 1.4$ S/m.

Recently, this approach has been extended to the general 3-D problem by Tsai [34]. Solutions obtained with this method have been found to agree well with the exact solution for homogeneous and concentrically layered spheres. Another method, developed by Schaubert *et al.* [35], uses the so-called rooftop functions which are linear in the normal direction and constant tangentially. This allows the normal $\overline{D}$ continuity to be enforced by constraint. The solutions obtained for spheres with this method are considerably superior to block model solutions. Two points stressed in these papers are that one, the cell structure of the model should accurately represent the dielectric interfaces and two, the linear basis is superior to the pulse basis in that it is capable of approximating the cell-to-cell boundary conditions more accurately. Both of these methods suffer, however, from two important limitations. The larger number of unknowns per cell results in a very large matrix equation to be solved. This makes the solution of high-resolution biological models beyond the reach of present-day computers. The other complication involves the creation of the model itself. The need to model interfaces accurately requires that the cell structure fit the complicated shape of the exterior boundary and the interior organs using arbitrary polyhedral cells. Specification of such a model thus requires a great deal of effort compared with the simple volume-averaged block models. At present, this appears to us to be a fundamental limitation of integral equation approaches. The FD-TD method, in contrast, does not seem to require accurate boundary specification. For this method, specification of the dielectric properties on a regular grid of points seems to be sufficient information to produce accurate solutions. In the next section, two modifications are made to the pulse-basis block model MoM that have been found to alleviate the convergence problems without going to a higher order basis function.

IV. A Modified Pulse-Basis MoM (MHFH)

To support the previous conjectures regarding the cause of the poor performance of the pulse-basis block model MoM, we now present two modifications that we have found to alleviate this problem for the TE case. The first modification was suggested in the last section—replace the block model with a model composed of irregularly shaped cells so that the curved boundaries are modeled accurately. An example of this improvement is shown in Fig. 13 for a circular cylinder. Two serious disadvantages resulting from this modification are one, as discussed previously, the creation of such models is considerably more difficult than the block models, and two, since the discretization grid is no longer square and of constant increment, the linear system no longer inherits the convolutional form of the integral equation. Thus, the discrete convolution theorem cannot be used and the order N^2 storage and order N^3 computation of matrix inversion are required. The second modification involves the accurate numerical evaluation of the second integral in (2). This integral represents an integration of the polarization charge that exists at the interface between two homogeneous regions with different dielectric properties. It is this polarization charge that accounts for the discontinuity of the normal component of the electric field at the interface. If a homogeneous region is subdivided into N subregions and the line integrals are

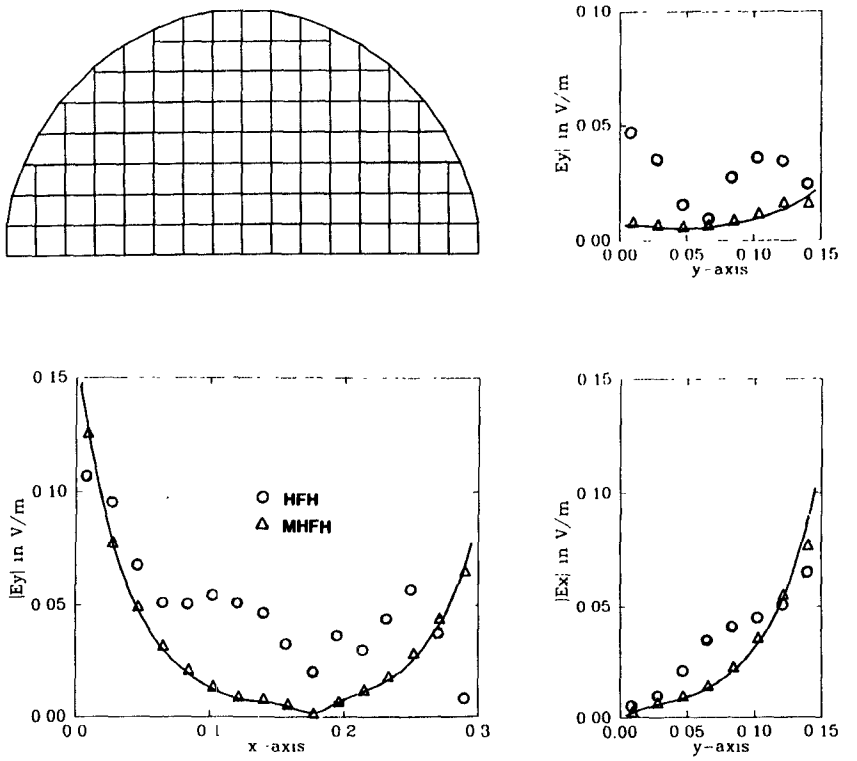

Fig. 13. Smooth model HFH and MHFH solutions versus the analytic solution. Frequency = 300 MHz, radius = 15 cm, $\epsilon_r = 54$, $\sigma = 1.4$ S/m.

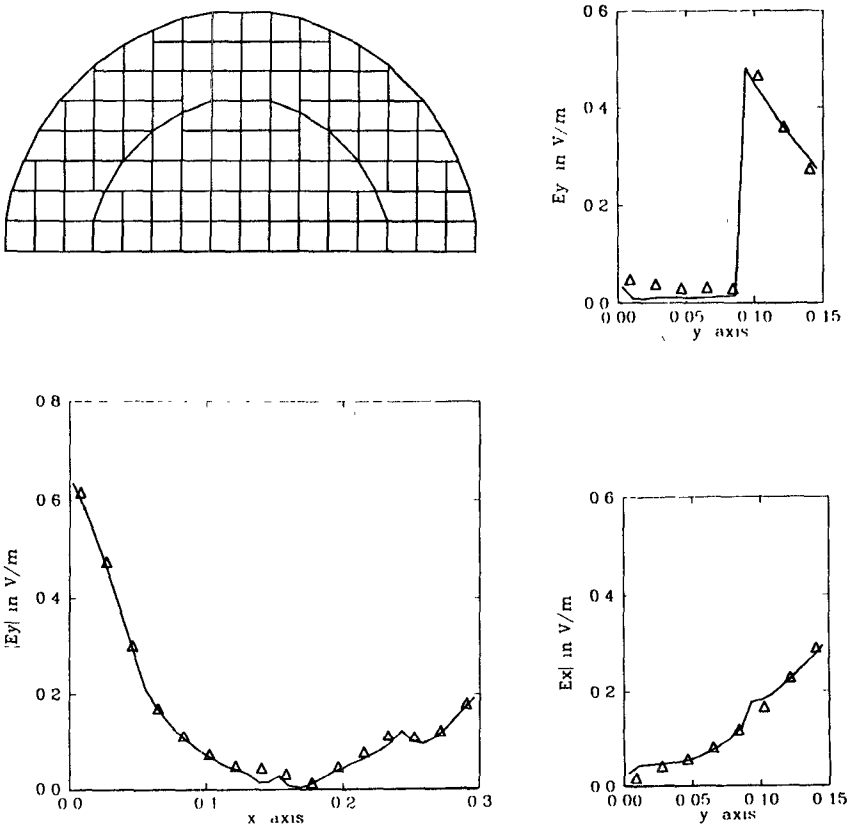

Fig. 14. Coaxially layered muscle-fat model and MHFH solution. Frequency = 300 MHz. Inner layer: radius = 9.4 cm, $\epsilon_r = 54$, $\sigma = 1.4$ S/m. Outer layer: radius = 15 cm, $\epsilon_r = 5.7$, $\sigma = 0.05$ S/m.

performed about the subregion boundaries, the continuity of normal $\bar{E}$ at the interface between two such subregions will ensure that the two integral contributions cancel so that the charge source exists only at the air–dielectric interface. The problem with the pulse basis is that, due to the assumption of constant fields, a jump discontinuity exists at all cell boundaries regardless of whether an actual dielectric discontinuity exists. This results in the presence of fictitious charge sources in the interior of the homogeneous regions. The second suggested modification is to ignore this deficiency of the pulse basis by simply not including the line integral contributions from cell boundaries for which there is not an actual dielectric discontinuity. Henceforth, this second modification shall be referred to as the modified high-frequency Hohmann method (MHFH) to differentiate it from the high-frequency Hohmann method (HFH) which includes the fictitious charge sources.

To examine the effects of these modifications, consider Fig. 12. Shown is a 208-cell block model of a homogeneous circular cylinder. One plane of symmetry has been used (as illustrated in the figure) to reduce the matrix size. The linear systems resulting from the HFH and MHFH were inverted by LU decomposition. The plots compare the two solutions with the exact solution as in previous examples. Notice that both solutions deviate significantly from the exact solution. Thus, the removal of fictitious charge alone is not sufficient to correct the solution.

Fig. 13 shows a smooth model created to satisfy the first suggested modification. The plots compare the solutions obtained with the HFH and MHFH methods. Clearly, modification of the boundary shape alone is not sufficient to correct the errors in the MoM solution. Notice, however, that if both modifications are made, the MoM solution agrees with the exact solution with very little error.

For an inhomogeneous test case, a 212-cell model of a coaxially layered circular cylinder was created, as shown in Fig. 14. Notice that both the exterior air–dielectric interface and the interior layer interface are accurately represented by the model. For the solution shown, the inner layer was assumed to be muscle surrounded by an outer layer of fat. Such a discontinuity represents the most severe case found in the human body. As in the homogeneous case, the MHFH method yields excellent agreement with the analytic solution. Note in particular the ability of the method to predict the large discontinuity in the E_y field at the interface along the y axis.

V. Conclusions

It has been shown that serious errors exist in solutions obtained using the HFH-MoM applied to block models of lossy dielectric cylinders for the TE polarization. The cause of these errors and their remedy have been demonstrated by the development of a modified HFH-MoM. In this method, the cell structure is designed to accurately model all dielectric interfaces. Also, the fictitious line charge sources present in the traditional HFH-MoM have been removed. Unfortunately, these modifications prevent the resulting linear system of equations from inheriting the convolutional form of the TE integral equation. This prevents the use of the FFT-CGM and thus requires the order N^2 storage and order N^3 computation of matrix inversion. Also, the need to include accurate interface modeling drastically increases the effort required to create models of complicated inhomogeneity as opposed to the simple volume-averaged models used in the past.

In contrast, the FD-TD method has been shown to yield excellent solutions for both the TM and TE polarizations without the need for accurate boundary information. This fact, coupled with the extreme efficiency in storage and computation requirements, suggests that the FD-TD method has great potential for solving the high-resolution models needed in bioelectromagnetics.

References

[1] H. Massoudi, C. H. Durney, P. W. Barber, and M. F. Iskander, "Electromagnetic absorption in multilayered cylindrical models of man," *IEEE Trans. Microwave Theory Tech.*, vol. MTT-27, pp. 825–830, Oct. 1979.

[2] W. T. Joines and R. J. Spiegel, "Resonance absorption of microwaves by the human skull," *IEEE Trans. Biomed. Eng.*, vol. BME-21, pp. 46–48, Jan. 1974.

[3] C. M. Weil, "Absorption characteristics of multilayered sphere models exposed to UHF/microwave radiation," *IEEE Trans. Biomed Eng.*, vol. BME-22, pp. 468–476, Nov. 1975.

[4] A. Lakhtakia, M. F. Iskander, and C. H. Durney, "An iterative extended boundary condition method for solving the absorption characteristics of lossy dielectric objects of large aspect ratios," *IEEE Trans. Microwave Theory Tech.*, vol. MTT-31, pp. 640–647, Aug. 1983.

[5] M. A. Morgan and K. K. Mei, "Finite-element computation of scattering by inhomogeneous penetrable bodies of revolution," *IEEE Trans. Antennas Propagat.*, vol. AP-27, pp. 202–214, Mar. 1979.

[6] J. H. Richmond, "Scattering by a dielectric cylinder of arbitrary cross section shape," *IEEE Trans. Antennas Propagat.*, vol. AP-13, pp. 334–341, Mar. 1965.

[7] J. H. Richmond, "TE wave scattering by a dielectric cylinder of arbitrary cross-section shape," *IEEE Trans. Antennas Propagat.*, vol. AP-14, pp. 460–464, July 1966.

[8] D. E. Livesay and K. M. Chen, "Electromagnetic fields induced inside arbitrarily shaped biological bodies," *IEEE Trans. Microwave Theory Tech.*, vol. MTT-22, pp. 1273–1280, Dec. 1974.

[9] M. J. Hagmann, O. P. Gandhi, and C. H. Durney, "Numerical calculation of electromagnetic energy deposition for a realistic model of man," *IEEE Trans. Microwave Theory Tech.*, vol. MTT-27, pp. 804–809, Sept. 1979.

[10] J. F. Deford, O. P. Gandhi, and M. J. Hagmann, "Moment-method solutions and SAR calculations for inhomogeneous models of man with large number of cells," *IEEE Trans. Microwave Theory Tech.*, vol. MTT-31, pp. 848–851, Oct. 1983.

[11] N. N. Bojarski, "K-space formulation of the electromagnetic scattering problem," Tech. Rep. AFAL-TR-71-5, Mar. 1971.

[12] R. Kastner and R. Mittra, "A new stacked two-dimensional spectral iteration technique (SIT) for analyzing microwave power deposition in biological media," *IEEE Trans. Microwave Theory Tech.*, vol. MTT-31, pp. 898–904, Nov. 1983.

[13] D. T. Borup and O. P. Gandhi, "Fast-Fourier-transform method for the calculation of SAR distributions in finely discretized models of biological bodies," *IEEE Trans. Microwave Theory Tech.*, vol. MTT-32, pp. 355–360, Apr. 1984.

[14] D. T. Borup and O. P. Gandhi, "Calculation of high-resolution SAR distributions in biological bodies using the FFT algorithm and the conjugate gradient method," *IEEE Trans. Microwave Theory Tech.*, vol. MTT-33, pp. 417–419, May 1985.

[15] M. Hestenes and E. Stiefel, "Method of conjugate gradients for solving linear systems," *J. Res. Nat. Bur. Stand.*, vol. 49, pp. 409–436, 1952.

[16] H. Massoudi, C. H. Durney, and M. F. Iskander, "Limitations of the cubical block model of man in calculating SAR distributions,"

IEEE Trans. Microwave Theory Tech., vol. MTT-32, pp. 746–752, Aug. 1984.
[17] M. J. Hagmann *et al.*, "Comments on 'Limitations of the cubical block model of man in calculating SAR distributions'," *IEEE Trans. Microwave Theory Tech.*, vol. MTT-33, pp. 347–350, Apr. 1985.
[18] K. S. Yee, "Numerical solution of initial boundary value problems involving Maxwell's equations in isotropic media," *IEEE Trans. Antennas Propagat.*, vol. AP-17, pp. 585–589, May 1966.
[19] A. Taflove and M. E. Morris, "Numerical solution of steady-state electromagnetic scattering problems using the time-dependent Maxwell's equations," *IEEE Trans. Microwave Theory Tech.*, vol. MTT-23, pp. 623–660, Aug. 1975.
[20] K. Umashankar and A. Taflove, "A novel method to analyze electromagnetic scattering of complex objects," *IEEE Trans. Electromagn. Compat.*, vol. EMC-24, pp. 397–405, Nov. 1982.
[21] A. Taflove and M. E. Brodwin, "Computation of the electromagnetic fields and induced temperatures within a model of the microwave-irradiated human eye," *IEEE Trans. Microwave Theory Tech.*, vol. MTT-23, pp. 888–896, Nov. 1975.
[22] G. Mur, "Absorbing boundary conditions for the finite-difference approximation of the time-domain electromagnetic-field equations," *IEEE Trans. Electromagn. Compat.*, vol. EMC-23, pp. 377–382, Nov. 1981.
[23] A. Taflove and K. R. Umashankar, "User's code for FD-TD," Final Report RADC-TR-82-16 by IIT Research Institute, Chicago, IL, to Rome Air Development Center, Griffiss AFB, NY, on Contract F30602-80-C-0302, Feb. 1982.
[24] R. F. Harrington, *Field Computation by Moment Methods*. New York: McGraw-Hill, 1968.
[25] G. W. Hohmann, "Three-dimensional induced polarization and electromagnetic modeling," *Geophysics*, vol. 40, pp. 309–324, Apr. 1975.
[26] M. J. Hagmann and R. L. Levin, "Convergence of local and average values in three-dimensional moment-method solutions," *IEEE Trans. Microwave Theory Tech.*, vol. MTT-33, pp. 649–654, July 1985.
[27] A. V. Oppenheim and R. W. Schafer, *Digital Signal Processing*. Englewood Cliffs, NJ: Prentice-Hall, 1975.
[28] T. K. Sarkar, K. R. Siarkiewicz, and R. F. Stratton, "Survey of numerical methods for solution of large systems of linear equations for electromagnetic field problems," *IEEE Trans. Antennas Propagat.*, vol. AP-29, pp. 847–856, Nov. 1981.
[29] P. M. Van den Berg, "Iterative computational techniques in scattering based on the integrated square error criterion," *IEEE Trans. Antennas Propagat.*, vol. AP-32, pp. 1063–1071, Oct. 1984.
[30] M. F. Sultan and R. Mittra, "An iterative moment method for analyzing the electromagnetic field distribution inside inhomogeneous lossy dielectric objects," *IEEE Trans. Microwave Theory Tech.*, vol. MTT-33, pp. 163–168, Feb. 1985.
[31] C. C. Johnson and A. W. Guy, "Nonionizing electromagnetic wave effects in biological materials and systems," *Proc. IEEE*, vol. 60, pp. 692–718, June 1972.
[32] H. E. Bussey and J. H. Richmond, "Scattering by a lossy dielectric circular cylindrical multilayer, numerical values," *IEEE Trans. Antennas Propagat.*, vol. AP-23, pp. 723–725, Sept. 1975.
[33] S. C. Hill, C. H. Durney, and D. A. Chistensen, "Numerical calculations of low-frequency TE fields in arbitrarily shaped inhomogeneous lossy dielectric cylinders," *Radio Sci.*, vol. 18, pp. 328–336, May–June 1983.
[34] C-T. Tsai, "Numerical studies of internal field distributions in dielectric bodies," Ph.D dissertation, University of Utah, Salt Lake City, UT, 1985.
[35] D. H. Schaubert, D. R. Wilton, and A. W. Glisson, "A tetrahedral modeling method for electromagnetic scattering by arbitrarily shaped inhomogeneous dielectric bodies," *IEEE Trans. Antennas Propagat.*, vol. AP-32, pp. 77–85, Jan. 1984.

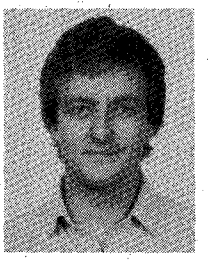

David T. Borup was born in Boise, ID, on October 24, 1958. He received the B.S. degree in mathematics from the College of Idaho, Caldwell, ID, in 1985. He is currently working toward the Ph.D. degree in electrical engineering at the University of Utah.

✠

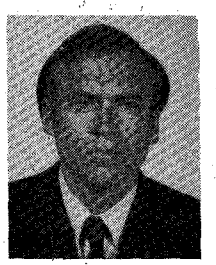

Dennis M. Sullivan was born in Madison, WI, on January 3, 1949. He received the B.S. degree in electrical engineering from the University of Illinois, Urbana, in 1973, and the M.S. degree in electrical engineering in 1978 and the M.E. degree in computer science in 1980, both from the University of Utah, Salt Lake City. He is now working toward the Ph.D. degree at the University of Utah.

✠

Om P. Gandhi (S'57–M'58–SM'65–F'79) received the B.Sc. degree (with honors) in physics from Delhi University, Delhi, India, and the M.S.E. and Sc.D. degrees in electrical engineering from the University of Michigan, Ann Arbor.

He is a Professor of Electrical Engineering at the University of Utah, Salt Lake City. He is the author or coauthor of one technical book and over 120 journal articles on microwave tubes, solid-state devices, and electromagnetic dosimetry, and he has recently written the textbook *Microwave Engineering and Applications* (Pergamon). He has been a principal investigator on over two dozen federally funded research projects since 1970, and serves or has served as a consultant to several government agencies and private industries.

Dr. Gandhi received the Distinguished Research Award of the University of Utah for 1979–1980 and a special award for "Outstanding Technical Achievement" from the Institute of Electrical and Electronics Engineers, Utah Section, in 1975. He edited the special issue (January 1980) of the PROCEEDINGS OF THE IEEE on Biological Effects and Medical Applications of Electromagnetic Energy. He is a past Chairman of the IEEE Committee on Man and Radiation (COMAR). His name is listed in *Who's Who in America*, *Who's Who in Engineering*, and *Who's Who in Technology Today*.